

PAPER • OPEN ACCESS

Ultrasonic Evaluation at the Interface of Aluminum/Steel Obtained by TIG Welding

To cite this article: Qumrul Ahsan and Hiroshi Kato 2019 *IOP Conf. Ser.: Mater. Sci. Eng.* **554** 012010

View the [article online](#) for updates and enhancements.

Ultrasonic Evaluation at the Interface of Aluminum/Steel Obtained by TIG Welding

Qumrul Ahsan¹ & Hiroshi Kato²

¹Carbon Research Technology Group, Advanced Manufacturing Centre, Faculty of Manufacturing Engineering, Universiti Teknikal Malaysia Melaka, Hang Tuah Jaya, 76100 Durian Tunggal, Melaka, Malaysia.

²Department of Mechanical Engineering, Division of Mechanical Science and Engineering, Saitama University, 255 Shimo-Okubo, Sakura-ku, Saitama-city, Saitama 338-8570, Japan

Corresponding author, email: qumrul@utem.edu.my

Abstract. Aluminum filler (Al-5%Si) is bonded on steel substrate by gas tungsten arc welding process under different current setting conditions. After welding a thorough metallographic analyses using optical and scanning electron microscopy were carried out to observe Al-Steel interface. Ultrasonic measurements by immersion and scanning acoustic microscopy were made to characterise the bond at Al-Steel interface. The ultrasonic wave reflected from the Al-Steel interface clearly indicated the more debonded area when the welding current is changed from direct current straight polarity (DCSP) mode to alternate current high frequency (ACHF) or the welding current in case of current for DCSP mode is reduced. This may be attributed either adequate amount of oxides along with intermediate phase make the bond interface rough and uneven due to introduction of ACHF mode or debonded areas are higher due to lower heat input when the current reduced to 125 amps from 150 amps in DCSP mode. Whereas smooth and even bond interface due to uniform heat input resulted stable Al-Steel interface and the mapping of bonded area by ultrasonic measurement showed spectrum of minimum peak for using current of 150 amps in DC mode. Thus the non-destructive assessments of interface between dissimilar materials through ultrasonic measurements could be important tools for evaluating the state of the bond.

1. Introduction

Aluminum and its alloys are widely used in fabrications because of their lightweight, good corrosion resistance and weldability. The unique combination of light weight and relatively high strength makes aluminum the second most popular metal that is welded. Light weight engineering structures are the prime concerns for automobile and shipbuilding industries. To reduce the weight of the structural components the combination of steel and aluminum alloy fabrication is considered to be an efficient measure. Several welding methods viz. explosive bonding or rolling [1] solid-phase bonding methods, such as friction welding [2], ultrasonic joining [3], rolling [4] and laser method [5, 6] are being utilized to join steel and aluminum. The investigations made by Yan et al. [5] clearly indicated the microstructural segregation at the interface of steel-Al joints clearly produced Fe-Al intermetallic compounds (IMCs), such as Fe₂Al₅, FeAl₃ and FeAl, that may improve the hardness of the interface layer dramatically but



reduce and ductility of weldment with increased susceptibility of solidification cracking in the fusion zone. Studies on friction stir welding (FSW) [7-11] for steel/aluminum weld have also been reported and the results show that the FSW joints exhibit superior mechanical and chemical properties compared to gas tungsten arc welding (GTAW) joints due to the presence of finer grains the weld metal of FSW joints. Many attempts have also been made so far to deposit aluminum alloy on commercial grade steel substrates by fusion welding process [12, 13]. Studies from Pouranvari et.al [12] indicated that low heat input rate of GTAW process reduce the growth of intermetallic compounds during joining. In a different study Su et. al. [13] prepared Al-steel lap joints from direct-current pulsed gas metal arc welding (DPG) and alternate-current double-pulse gas metal arc welding (ADG) and showed that ADG process offers higher joint strength than that offered by DPG process due to thinner intermetallic compounds layer resulted from lower heat input.

However, sound joints are difficult to produce, because hard and brittle intermetallic compounds are formed at the weld whenever steel is welded to aluminum by fusion welding. The reason for this is attributed to the large difference between their melting points (933 K for Al and 1811 K for Fe), the very few solid solubility of iron in aluminum, and the formation of brittle intermetallic compounds such as Fe_2Al_5 and FeAl_3 [14]. Further, differences in their thermal properties like expansion coefficients, conductivities, and specific heats lead to internal stresses after fusion welding. In addition, presence of oxide layers during welding at steel aluminum interface can cause debonding. Therefore, fusion welds of iron and aluminum suffer from cracking with brittle failure in service [14]. Quality control of steel-aluminum weldment is considered as the prime concern for the fabrication industries. Tools and techniques especially utilization of ultrasound in non-destructive evaluation is widely used to ensure the proper quality of the weldment.

Cracks, formation of pores and other discontinuities in deposit are also of great concern to determine. A very efficient method for detecting these defects and measuring layer thickness is the ultrasonic method [15] and this can lead to strong effects on the ultrasonic properties. Hudgell [16] gave a description of austenitic clad components and of the ultrasonic testing of such components. Investigations into the energy aspect of the reflectivity for the lamination-type flaws show that the energy reflected depends on the specific wave resistance of the layers involved and the kind of substance filling the space between them, as well as on the ratio of flaw thickness and ultrasonic wave length. Generally, in the case of flaws of delamination type, the reflectivity increases and this increase is used as the basis for the ultrasonic flaw detection methods.

In the present work, ultrasonic measurements were carried out to evaluate the bond interface of steel and aluminum at different welding conditions. Welding in steel substrate with Al-5% Si alloy as filler is manually carried out at different current settings under constant welding speed through welding torch. Studies have been carried out to obtain the relationships between the state of the bonding interface and ultrasonic parameters, such as the transmissibility (or reflectivity) of an ultrasonic wave at the bonding interface and an ultrasonic waveform traveling through the interface.

2. Experimental

2.1. Preparation of specimen

In this study, steel plates were used to make weld bead deposit of Al alloy on it. The chemical analysis of the plate was carried out by optical emission spectroscopy (OES) and the result found from OES is given in Table 1. From the OES result, it was found that the steel plate is simple grade of mild steel. The mild steel plates were machined to the required dimensions of 75 mm × 50 mm × 8 mm. First the contaminants and oxide film on the steel surface were removed by steel brush. Final cleaning of the steel faying surface was carried out by acid pickling using 5% hydrochloric acid for 10-12 minutes.

Table 1. Chemical composition in wt.% of steel plate and Al filler used in this investigation. (OES)

Materials	Elements (in wt. %)					
	C	Si	Mn	Cu	Fe	Al
Mild Steel Plate	0.13	0.09	0.5	<0.01	bal	
Al-4043 filler	-	4.5 - 5.0	-	<0.3	-	bal

An A4043 (Al-5%Si) grade filler rod was used for gas tungsten arc welding (GTAW) process, and single pass welding was used to deposit aluminum weld bead on steel surface. The welding procedure was carried out by a certified welder. The plates were clamped and welded manually in the flat position using Al-5% Si filler metals at different welding currents with constant welding speed. High purity (99.99%) argon shielding gas with a flow rate of 15 liter/min was used in all welding trials. The welding current modes for ACHF and DCSP with welding parameters are presented in Table 2 to fabricate aluminum-steel (Al/Steel) clad in this study. Usually DC welding is the preferred type of welding either using direct current straight polarity (electrode negative) or direct current reverse polarity (electrode positive) to produce a smoother weld than AC. As DC delivers a constant and consistent current it is expected that welding of aluminum on steel substrate may produce a smoother interface with thin intermetallic layer. Whereas, when using AC, the current swings with changing polarity and causing fluctuation in arc which may disrupt the aluminum steel interface with higher chance of making the bond interface rough and uneven. The welding heat input rate (Q_w) for both DCSP and ACHF was calculated using following formula [17]:

$$Q_w = \frac{\eta VI}{S} \quad (1)$$

where, V is the arc voltage, I is the welding current, S is the welding speed (measured as the welding length divided by the welding time) and η is arc efficiency (considered as 0.6, a typical value for GTAW process [17]).

Table 2. Welding conditions and process parameters

Sample ID	Welding Process	Welding Mode	Current Freq. (Hz)	Average Voltage (V)	Average Current (A)	Welding Speed S (mm/min)	Heat Input Q_w (kJ/mm)
ACHF 150	GTAW	ACHF	50	15	150	60	540
DCSP 150	GTAW	DCSP	-	15	150	60	540
DCSP 125	GTAW	DCSP	-	15	125	60	450

After welding, the welded plates were cooled in air. Aluminum weld deposit for each sample was machined by milling cutter to make it around 2 mm thick. The steel substrate of each sample was also machined to make smooth and parallel surface with aluminum surface, and the thickness of the steel was made to around 7 mm thick.

2.2. Ultrasonic measurement

In order to characterize the aluminum-steel interface, the ultrasonic measurement by immersion method and the scanning acoustic microscope along were used. An experimental setup of ultrasonic measurement by immersion methods is shown in Fig. 1. The transducer of 10 mm diameter generating a longitudinal wave of 20 MHz in frequency with a focal distance of 25.4 mm in water was used. A distance between the transducer and the specimen (water path) was controlled so that the ultrasonic

wave was focused at the steel–aluminum interface. In each sample, the ultrasonic measurement was carried out at 10 x 10 scanning points in an area of 9 x 9 mm with a pitch of 1 mm by irradiating the ultrasonic wave from steel side, whereas scans were made on 20 points in a linear distance with a pitch of 1 mm from the aluminum side for same sample. In this method, the probe was kept constant distance from the surface of the object to be inspected, and scanned the surface to detect irregularities of the interface.

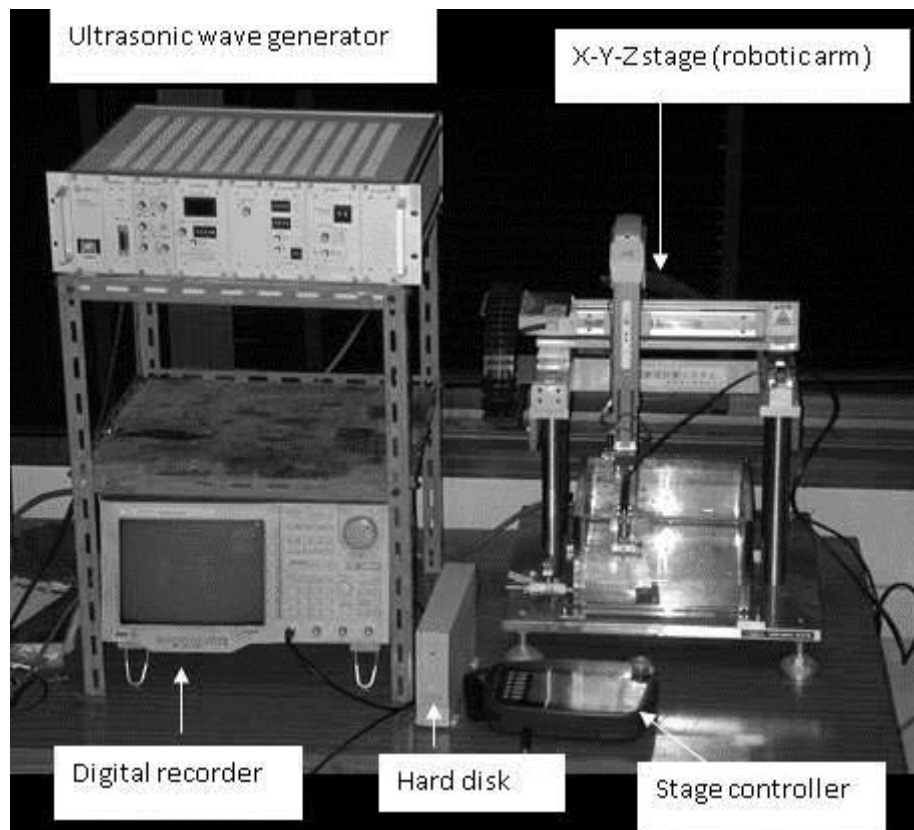


Figure 1. Experimental set up of ultrasonic C-scan system for immersion scanning.

Scanning acoustic microscope (SAM) as shown in Fig. 2 was used to obtain acoustic intensity image from the aluminum side with a probe generating a wave of 50 MHz in frequency with a focal distance of 10 mm in water to produce high resolution images at the aluminum-steel interface, and interfacial separation and irregularities at weld interface were detected. In the present analysis, the maps of an area of 18 mm x 18 mm were obtained at six different locations and combined for each sample. The absolute value of the highest amplitude signal within the gated region was recorded.

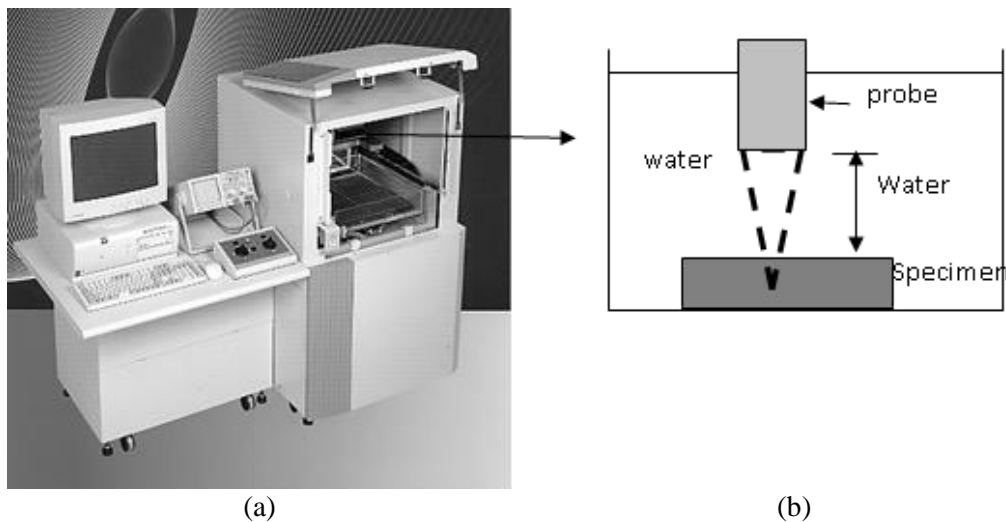


Figure 2. (a) Scanning Acoustic Microscope and (b) specimen and probe position in the water.

2.3. Metallography

After ultrasonic inspection, samples were cut into small sections. Then the sections were mounted in epoxy resin under pressure. Optical metallography was performed on all specimens. Before metallography, specimens were longitudinally sectioned and prepared as per the standard metallographic practice. Polishing was carried out using emery paper of various grades. Finally, wheel polishing was done with gamma alumina and water as lubricant. The samples were then etched with nital. Relevant microstructures at the various locations of the aluminum weld deposit, weld (Al)-substrate (steel) and the steel substrate were observed under optical microscope.

All metallographic surfaces were also observed under scanning electron microscope (SEM). The SEM micrographs were obtained from secondary electron and back scattered electron images at around 10 kV. Qualitative composition measurements of the elements at the weld substrate interface were conducted by energy dispersive X-ray analysis (EDX) at 10 kV.

3. Results and Discussion

3.1. Interfacial structures

In this section, features of the interfacial structures are shown and discussed on the relation between the welding conditions and the morphology of the interface, formation of the intermetallic compound layer. The interfacial structures are shown in Fig. 3(a), (b) and (c) for ACHF 150 sample and the optical micrographs [Fig. 3(a)] of aluminum weld deposit shows wavy surface at steel substrate. A layer of intermetallic compound and large amount of oxides on weld deposit are also observed. In scanning electron micrographs, a layer of intermetallic compound (Fe_2Al_5) is also clearly observed in Fig. 3(b) and the intermetallic compound of different compositions can be attributed from back scattered electron image [Fig. 3(c)]. Delamination due to poor bonding at steel substrate and aluminum weld deposit are also found in SEM. EDX were carried out at weld deposit, interface and substrate and analysis clearly shows the dilution of Al due to its presence at interface [Fig. 4]. For weld deposits made from DCSP with current settings of 150 Amp, no delamination or poor bonding was observed in optical and scanning electron micrographs for DCSP 150 [Fig. 5] but in DCSP 125 [Fig. 6] some poor bonding at different regions of interface are located.

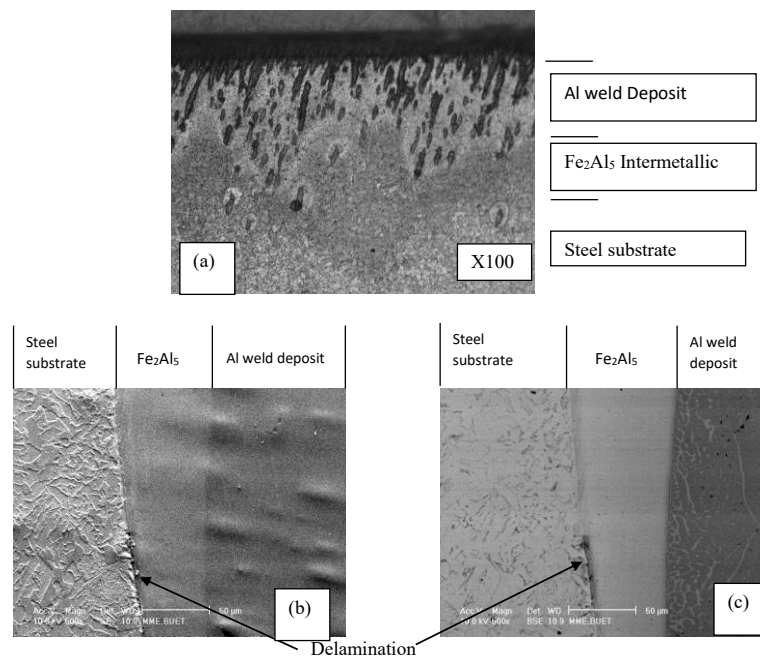


Figure 3. Optical micrograph of ACHF 150 at Al-Steel interface (a), scanning electron micrographs of same region for secondary electron (b) and back scatter electron detection mode (c).

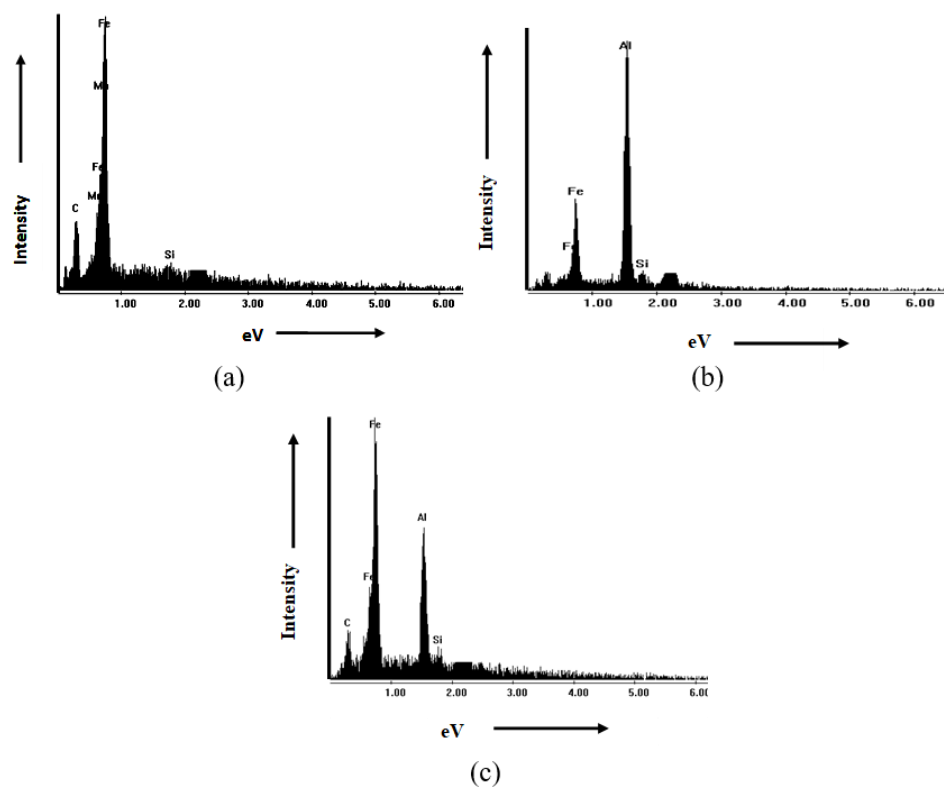


Figure 4. EDX spectra of (a) Steel substrate (b) Al weld deposit and (c) Al/Steel Interface of ACHF 150 sample.

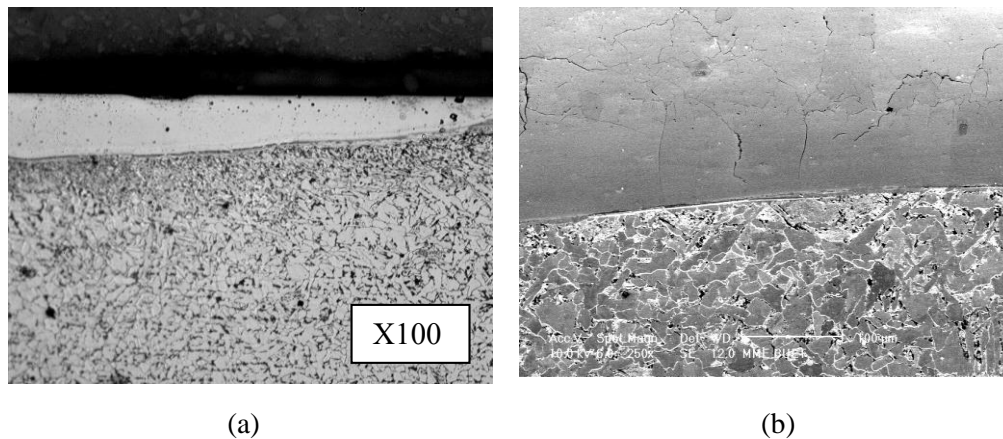


Figure 5. (a) Optical micrograph of Al-Steel interface of DCSP 150 sample and (b) scanning electron micrographs of same region.

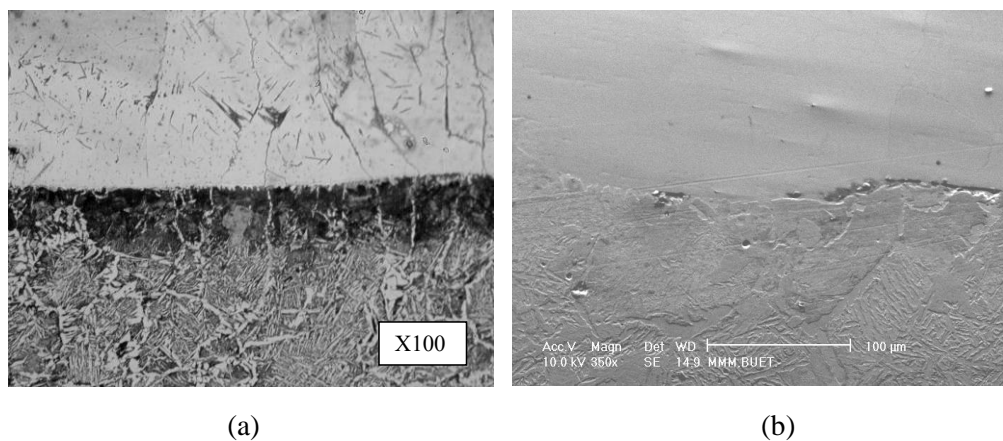


Figure 6. (a) Optical micrograph of Al-Steel interface of DCSP 125 sample and (b) scanning electron micrographs of same region.

3.2. Relation between ultrasonic wave intensity and irregularity of interface

In this part, the results of the ultrasonic measurement are shown, and the relation between the ultrasonic wave reflected from the surface, the interface and the bottom and the features of the interface are discussed. In immersion method ultrasonic scanning were carried out from both the steel side and aluminum side for three different weld conditions. In order to determine the reflection nature from interfaces the acoustic impedances and the calculated reflected wave ratios at different interfaces are given in Table 3.

Table 3. Acoustic impedance and reflected wave ratios at different interfaces.

Acoustic Impedance, kg/m ² -s			Reflected wave ratio at interface of		
Water (W)	Steel (S)	Aluminum (Al)	W/S	S/Al	Al/W
1.50 x 10 ⁶	4.54 x 10 ⁷	1.71 x 10 ⁷	0.936	-0.453	-0.839

In case of weld deposit made from ACHF 150, the ultrasonic scanning reflection patterns from steel and aluminum sides are shown in Fig 7 (a) and (b) respectively. From steel side the first peak echo at water/steel (W/S) interface is negative whereas, the peak echoes from steel/Al (S/A) and Al/water (A/W) interfaces are positive as the reflected wave ratios for W/S is positive and for S/A and A/W are negative

(Table 3). When the same sample is scanned from aluminum side amplitude of reflected echo from aluminum/steel (A/S) interface [Fig. 7(b)] is almost half of the echo obtained at steel/aluminum interface [Fig. 7(a)] although the reflected echo is almost 50% of the incident echo. This can be explained from the micrographs obtained from optical and scanning electron micrographs (Fig. 3). In optical micrographs [Fig. 3(a)] aluminum weld deposit makes wavy surface at steel substrate. A layer of intermetallic compound and large amount of oxides on weld deposit are also observed. Usually it is reported [18] when a smooth layer of intermetallic was formed, echo reflectivity was in good agreement with the theoretical value whereas, the non-uniform layer caused rough interface due to presence of oxides and the ultrasonic wave was largely scattered at the interface with echo reflectivity decreased below the theoretical value. At present echo reflectivity showed large scattering for ACHF 150 sample and this may due to large amount of oxide may cause poor bonding at steel aluminum interface. In scanning electron micrographs, a thick layer of intermetallic compound (Fe_2Al_5) was also clearly observed [Fig. 3(b)] and the intermetallic compound of different compositions can be attributed from back scattered electron image [Fig. 3(c)]. Delamination due to poor bonding at steel substrate and aluminum weld deposit are also found in SEM. EDX were carried out at weld deposit, interface and substrate and analysis clearly shows the dilution of Al due to its presence at interface [Fig. 4].

During ultrasonic scanning from steel side, these delamination may cause big reflection [Fig. 7(a)] due to presence of air between the steel and aluminum as the reflectivity at steel/air is almost -1 due to acoustic impedance of the air is very small. Whereas, when the ultrasonic scanning was carried out from Al side reflections may occur from Al/ Fe_2Al_5 and from delamination at close proximity. As a result, instead of sharp peaks, reflections peaks became broader with low amplitude.

For weld deposits made from DCSP with current settings of 150 amps, the scanning reflection patterns from steel and aluminum sides for same sample are shown in Fig 8(a) and (b) respectively. In general, reflected echoes for DCSP 150 from S/Al interface are of smaller height as compared to ACHF 150 but in some scanning points of DCSP 150 showed similar echo pattern as of ACHF 150. No delamination or poor bonding was observed in optical and scanning electron micrographs for DCSP 150 [Fig. 5] but in DCSP 125 [Fig. 6] some debonding at different regions of interface were located.

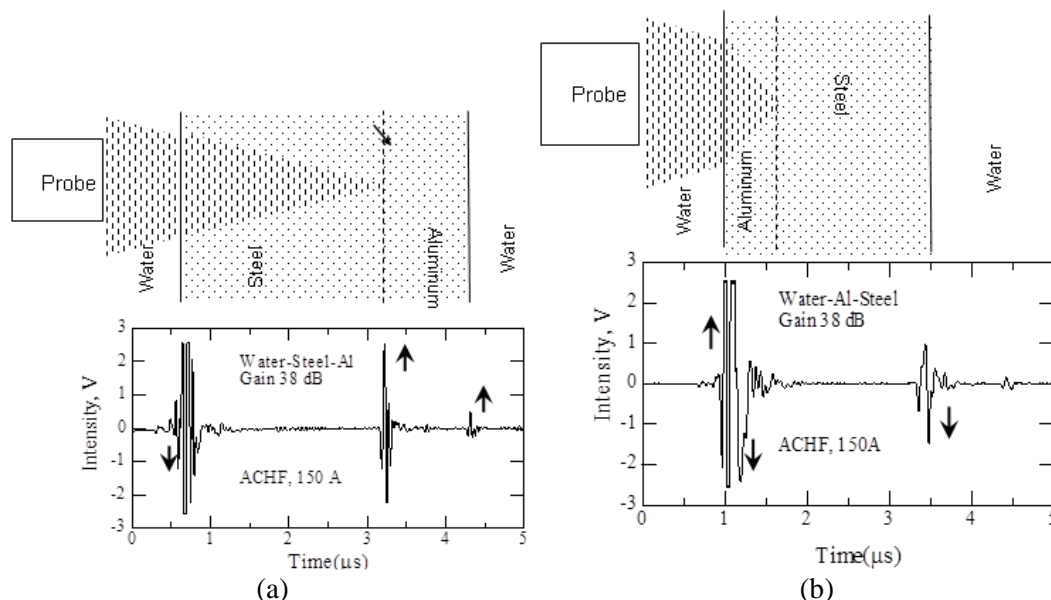


Figure 7. Ultrasonic wave reflection patterns of ACHF 150. Scanning from (a) steel side and (b) aluminum side in immersion method.

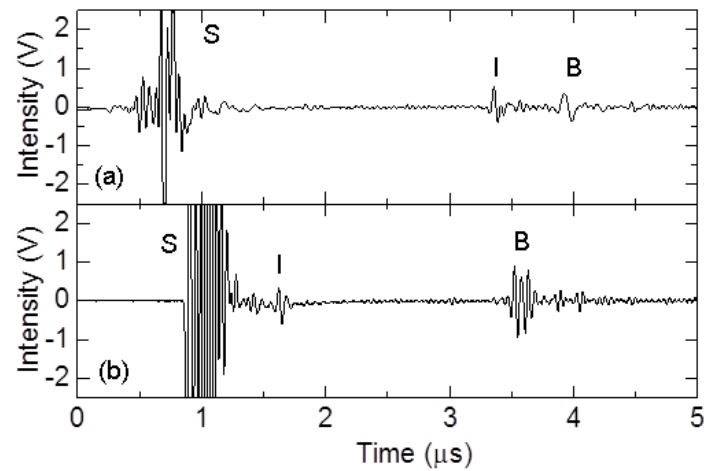
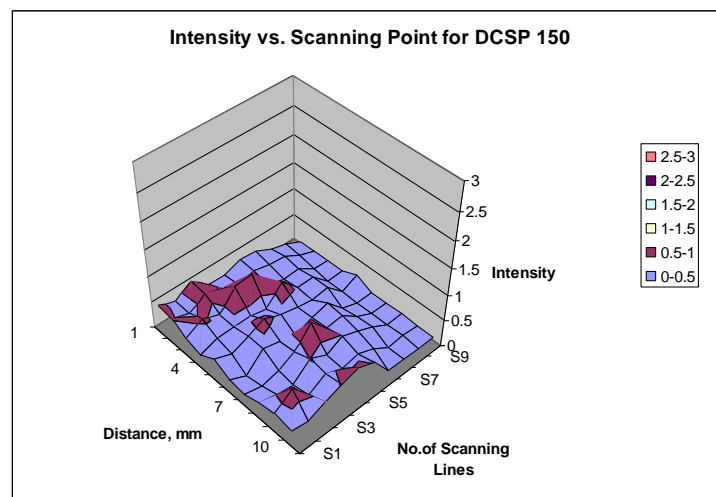


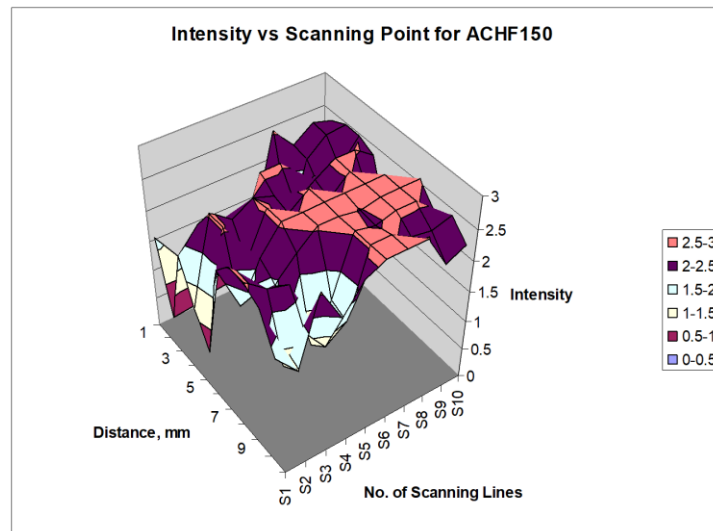
Figure 8. Ultrasonic wave reflection patterns of DCSP 150. Scanning from (a) steel side and (b) aluminum side in immersion method. (S-surface, I-Interface and B-Back surface)

3.3. Mapping of the intensity of echo reflected from welding interface

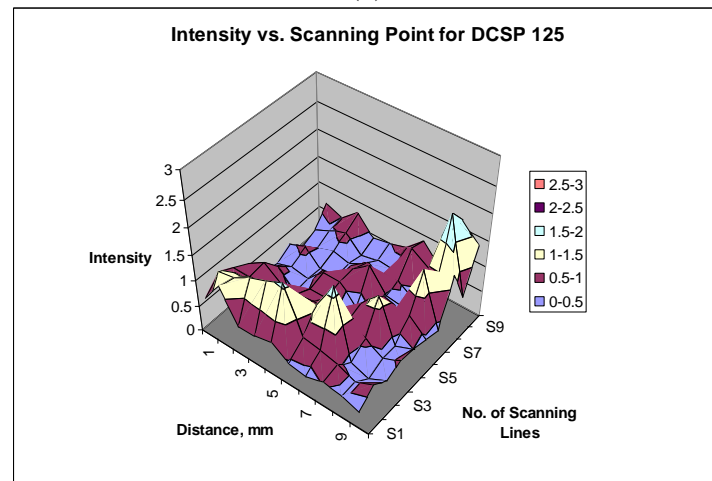
Maps of ultrasonic intensity reflected from the interface obtained by the ultrasonic measurement and also by the scanning acoustic microscope are shown to discuss the relation between the intensity distribution and the bonding conditions. In order to assess the total scanned interfaces of three samples, reflection values at interfaces versus scanning points are plotted and these are shown in Fig. 9. It is clear from these figures that the highest reflection intensities were obtained in ACHF 150, moderate reflection intensities in DCSP 125 and the minimum reflection intensities in DCSP 150.



(a)



(b)



(c)

Figure 9. Mapping of reflected ultrasound echo intensities from (a) ACHF 150, (b) DCSP 150 and (c) DCSP 125 samples in C-scan immersion method.

Finally, bonding conditions of aluminum weld deposits on steel substrates were characterized by scanning acoustic microscope (SAM) with a probe of 50 MHz in order to locate the debonding areas by taking images of aluminum-steel interfaces of three samples. The large bright regions (white spots) in acoustic image were the debonding area as shown in Fig 10. The map of reflected waves gives an idea of how impedance changes within sample. This wave travels to the specimen through a medium or couplant, which is usually deionized water since sound waves could not travel through air at the frequencies used. The ultrasound wave energy traveled through the aluminum at the aluminum's velocity, with a portion of ultrasound energy being reflected back every time when it hit at the aluminum steel interface. ACHF 150 showed the large number of white spots clustered in some regions which are attributed to debonded area [Fig. 10(b)], whereas DCSP 125 revealed white spots in terms of reflection of sound rather scattered in a large area [Fig. 10(f)]. Scanning in DCHP 150 sample almost provided no indication of white spots [Fig. 10(d)] i.e. most of the ultrasound transmitted through the interface which matched with the scanned result of the immersion method as shown in Fig.9(b). As compared to interface images [Fig. 10(b), (d) and (f)], SAM images of the surfaces [Fig. 10(a), (c) and (e)] of three samples only revealed the surface profile of aluminum.

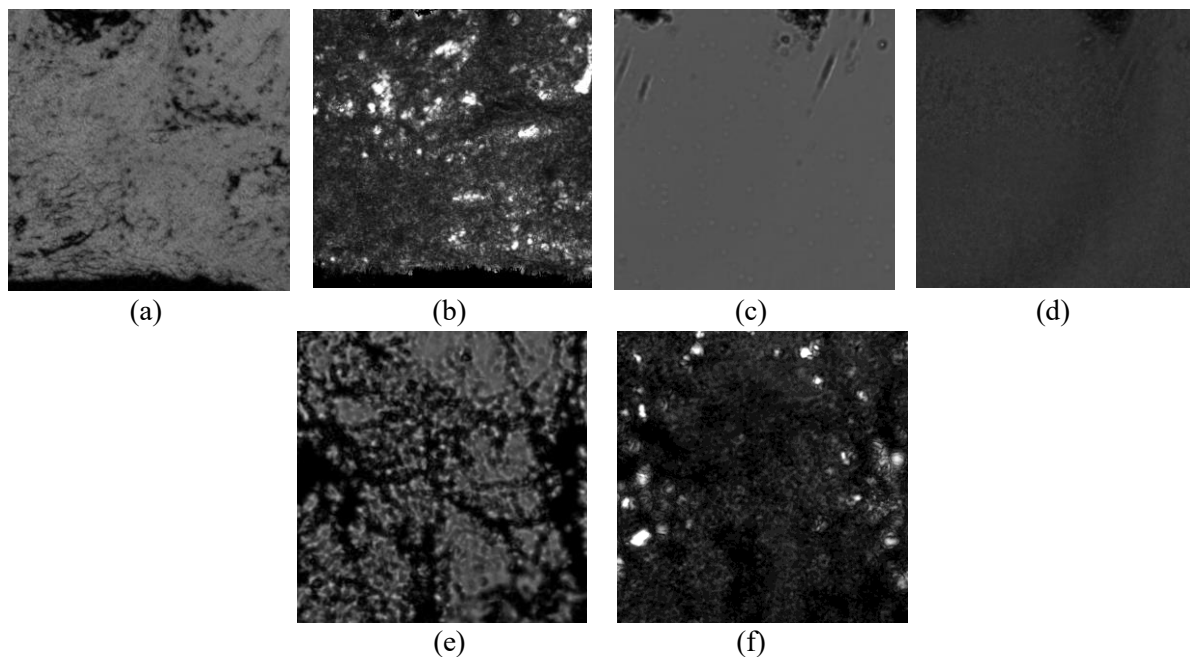


Figure 10. Scanning acoustic microscope images (a) from top and (b) at interface of ACHF 150, (c) from top and (d) at interface of DCSP 150 and (e) from top and (f) at interface of DCSP 125.

4. Conclusions

In this paper, deposition and thus bonding of Al filler on steel substrate by GTAW process at different current settings were evaluated by ultrasound wave propagation studies. From this investigation, the following important conclusion has been derived:

Of the three welded bonds, the joint fabricated by ACHF 150 exhibited intrusion of oxides in bond layer and resulted wavy at Al-Steel interface. Waviness at interface caused weak bonding. Both the ultrasonic immersion-C scan and scanning acoustic microscopy show the maximum reflection in terms of echo height or white spot. Whereas for DCSP 150 where the heat input is maximum associated with stable arc causing good and smooth interface. During ultrasonic inspection DCSP 150 exhibited the minimum reflection resulted from strong bond at Al-Steel interface. When heat input is lower than the DCSP 150 i.e. for DCSP 125 bond at interface was rather poor but superior than the ACHF 150 where are instability occurred due to change of polarity during welding. Mapping of ultrasonic C-scanning and image from scanning acoustic microscopy can be used as both qualitative and quantitative tools for characterizing dissimilar metal weld.

Acknowledgement

We greatly acknowledge Universiti Teknikal Malaysia (UTeM) Melaka, Malaysia, Saitama University, Japan and Bangladesh University of Engineering and Technology (BUET) for sponsoring this work. One of the authors is grateful to the Division of Mechanical Science and Engineering, Saitama University for extending the facilities of laboratories and express his sincere thanks to Saitama University for the financial support to carry out this investigation under the cooperative research program.

References

- [1] Maruzen. 1990. Welding Handbook. Edited by Japan Welding Society: pp. 496.
- [2] Aritoshi, M., and Okita, K. 2002. Friction welding of dissimilar metals. J. of Japan Welding Society 71-6, pp.432–436.

- [3] Watanabe, T., and Yoneda, A., et al. 1999. A study on ultrasonic welding of dissimilar metals, 1st and 2nd reports. Quarterly J. of Japan Welding Society 17-5, pp. 223–242.
- [4] Kouno. 2002. Manufacture of Al/SUS clad by vacuum rolling joining method and its properties. J. Japan Welding Society 71-6, pp.427–431.
- [5] Yan, F., Fang, X. F., Chen, L., Wang, C. W., Zhao, J., Chai, F., and Wang, W. 2018. Microstructure evolution and phase transition at the interface of steel/Al dissimilar alloys during Nd: YAG laser welding. Optics and Laser Technology 108, pp 193–201.
- [6] Katayama, S. 2002. Dissimilar materials joining by laser. Welding Technology 50-2, pp 69–73.
- [7] Malarvizhi, S., and Balasubramanian, V. 2011. Effect of welding processes on AA2219 aluminium alloy joint properties. Trans. Nonferrous Met. Soc. China 21, pp 962-973.
- [8] Thomas, W. Metal. Friction stir welding, international patent application PCT/GB92/02203.
- [9] Watanabe, T., Takayama, H., and Kimapong, K. 2003. Joining of steel to aluminum alloy by interface-activated adhesion welding. Materials Science forum, 426-432, pp. 4129–4134.
- [10] Yoshikawa, K., and Hirano, T. 2001. Numerically controlled friction stir welding in layered dissimilar metal materials of aluminum and steel. Proceedings of the Third Symposium on Friction Stir Welding, Kobe, Japan, September, pp. 1–11.
- [11] Kimapong, K., and Watanabe T. 2004, Friction stir welding of aluminum alloy to steel, Welding Journal, Oct., pp 277 – 282.
- [12] Pouranvari, M., and Abbasi, M. 2018. Dissimilar gas tungsten arc weld-brazing of Al/steel using Al-Si filler metal: Microstructure and strengthening mechanisms. Journal of Alloys and Compounds 749, pp 121-127.
- [13] Su, Y., Hua, X., and Wu, Y. 2013. Effect of input current modes on intermetallic layer and mechanical property of aluminum–steel lap joint obtained by gas metal arc welding. Materials Science & Engineering A 578, pp 340–345.
- [14] Rathod, M. J., and Kutsuna M. 2004. Joining of aluminum alloy 5052 and low-carbon steel by laser roll welding. Welding Journal, Welding Research Supplement, pp 16-26 S.
- [15] Bobrov V. A., and Khimchenko N. V. 1971. Ultrasonic inspection of clad metals, UDC 620.179.16:62-419.4, Translated From Khimicheskoe I Neftyanoe Mashinstroenie, Aug, 1971, No. 8, pp 29-31.
- [16] Hudgell, R. J. 1994. Handbook on the ultrasonic examination of austenitic clad components, The International Institute of Welding and Joint Research Centre, European Commission, Luxembourg.
- [17] Kou, S. 2003. Welding Metallurgy, second ed., John Wiley & Sons, Inc., Hoboken, New Jersey.
- [18] Kato, H., Abe, S., and Tomizawa T. 1997. Interfacial structures and mechanical properties of steel–Ni and steel–Ti diffusion bonds. Journal of Materials Science 32, pp 5225 – 5232.